Whole-Body Biodistribution and Dosimetry of the Dopamine Transporter Radioligand ^{18}F-FE-PE2I in Human Subjects

Helena Lizana[1], Lennart Johansson[1], Jan Axelsson[1], Anne Larsson[1], Mattias Ögren[2], Jan Linder[3], Christer Halldin[4], Andrea Varrone[4], and Susanna Jakobson Mo[2]

[1]Radiation Physics, Department of Radiation Sciences, Umeå University, Umeå, Sweden; [2]Diagnostic Radiology, Department of Radiation Sciences, Umeå University, Umeå, Sweden; [3]Clinical Neuroscience, Department of Pharmacology and Clinical Neuroscience, Umeå University, Umeå, Sweden; and [4]Centre for Psychiatry Research, Department of Clinical Neuroscience, Karolinska Institutet, Stockholm, Sweden

^{18}F-(*E*)-*N*-(3-iodoprop-2-enyl)-2β-carbofluoroethoxy-3β-(4′-methylphenyl) nortropane (^{18}F-FE-PE2I) was recently developed and has shown adequate affinity and high selectivity for the dopamine transporter (DAT). Previous studies have shown promising results for ^{18}F-FE-PE2I as a suitable radioligand for DAT imaging. In this study, we investigated the whole-body biodistribution and dosimetry of ^{18}F-FE-PE2I in healthy volunteers to support its utility as a suitable PET imaging agent for the DAT. **Methods:** Five healthy volunteers were given a mean activity of 2.5 MBq/kg, and 3 PET scans, head to thigh, were performed immediately after injection followed by 4 whole-body PET/CT scans between 0.5 and 6 h after injection. Blood samples were drawn in connection with the whole-body scans, and all urine was collected until 6 h after injection. Volumes of interest were delineated around 17 organs on all images, and the areas under the time–activity curves were calculated to obtain the total number of decays in the organs. The absorbed doses to organs and the effective dose were calculated using the software IDAC. **Results:** The highest activity concentration was observed in the liver (0.9%–1.2% injected activity/100 g) up to 30 min after injection. At later time points, the highest concentration was seen in the gallbladder (1.1%–0.1% injected activity/100 g). The activity excreted with urine ranged between 23% and 34%, with a mean of 28%. The urinary bladder received the highest absorbed dose (119 μGy/MBq), followed by the liver (46 μGy/MBq). The effective dose was 23 μSv/MBq (range, 19–28 μSv/MBq), resulting in an effective dose of 4.6 mSv for an administered activity of 200 MBq. **Conclusion:** The effective dose is within the same order of magnitude as other commonly used PET imaging agents as well as DAT agents. The reasonable effective dose, together with the previously reported favorable characteristics for DAT imaging and quantification, indicates that ^{18}F-FE-PE2I is a suitable radioligand for DAT imaging.

Key Words: ^{18}F-FE-PE2I; dosimetry; biodistribution; DAT; effective dose

J Nucl Med 2018; 59:1275–1280
DOI: 10.2967/jnumed.117.197186

Dopamine transporter (DAT) imaging with SPECT is at present the most widely established nuclear medicine procedure to support the diagnosis of degenerative parkinsonism. ^{123}I-*N*-3-fluoropropyl-2β-carbomethoxy-3β-4-iodophenyl tropane (^{123}I-FP-CIT), or ioflupane, also known under the commercial name DaTSCAN (GE Healthcare), is the most commonly used imaging agent for DAT SPECT in the routine diagnostic workup of patients (*1*) and has also been approved in the European Union to support the differential diagnosis between dementia with Lewy bodies and Alzheimer disease (*2*). However, the currently established method has its limitations. One issue is that ^{123}I-FP-CIT is not selective for the DAT but also shows affinity for the serotonin transporters (*3*). Reduction of striatal and extrastriatal serotonin transporter availability has been found in Parkinson disease (*4*) and might affect the ^{123}I-FP-CIT uptake pattern, particularly in extrastriatal regions. The PET imaging technique is technically advantageous, with better resolution, sensitivity, and quantification than SPECT. These advantages can be especially beneficial in clinical imaging, where a high spatial and temporal resolution may be needed for quantitative analyses.

^{18}F-(*E*)-*N*-(3-iodoprop-2-enyl)-2β-carbofluoroethoxy-3β-(4′-methyl-phenyl) nortropane (^{18}F-FE-PE2I) is a recently developed radioligand that shows suitable characteristics for a DAT imaging tool both in nonhuman primates (NHPs) and in human subjects. The fast washout from the brain and the favorable metabolism make ^{18}F-FE-PE2I superior to other related PET radioligands (e.g., ^{11}C-PE2I and ^{18}F-FECNT) for DAT quantification (*5–7*). In addition, the relatively high specific-to-nondisplaceable binding ratio of ^{18}F-FE-PE2I permits quantification of the DAT also in extrastriatal regions, such as the substantia nigra, where the cell bodies of the dopaminergic neurons are located. This capability provides the possibility for in vivo visualization of the pathophysiology of Parkinson disease (*5,8*) and offers a high-quality DAT imaging option.

The first study, including 10 Parkinson disease patients and 10 age- and sex-matched control subjects, demonstrated the ability of ^{18}F-FE-PE2I to quantify the nigrostriatal DAT loss in Parkinson disease (*9*). Findings from further studies supported the use of ^{18}F-FE-PE2I as a diagnostic tool for the evaluation of parkinsonian patients in the clinical setting (*9–11*).

To further explore ^{18}F-FE-PE2I as a diagnostic imaging agent, it is important to study its distribution and radiation exposure in human subjects. During the preclinical development of the radioligand, the whole-body biodistribution and dosimetry of ^{18}F-FE-PE2I were

Received Jun. 7, 2017; revision accepted Dec. 30, 2017.
For correspondence or reprints contact: Helena Lizana, Radiation Physics, Centre for Biomedical Engineering and Radiation Physics, University Hospital of Umeå, 901 85 Umeå, Sweden.
E-mail: helena.lizana@vll.se
Published online Jan. 18, 2018.

examined in 2 NHPs. This permitted the first-in-humans (to our knowledge) validation of ^{18}F-FE-PE2I (*10*). The estimates of the effective dose based on biokinetic data from NHPs are usually considered predictive of the actual dose to human subjects, although some discrepancies can be expected (*11*). Therefore, a full evaluation of whole-body distribution and dosimetry in human subjects will be warranted before widespread application of the PET imaging agent.

The aim of this study was therefore to study the whole-body biodistribution of ^{18}F-FE-PE2I in human subjects and to calculate radiation exposure and effective dose. The hypothesis was that the radiation safety data previously obtained from NHPs would be confirmed in human subjects, supporting the utility of ^{18}F-FE-PE2I as a PET imaging agent for the DAT.

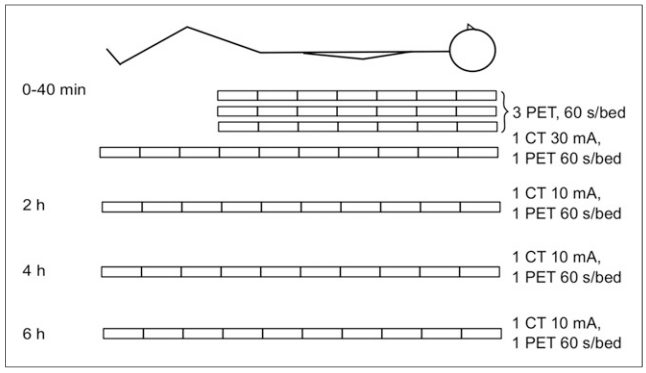

FIGURE 1. Illustration of PET/CT scanning protocol. All PET scans were performed with 60 s/bed position. Three head-to-thigh PET scans and one whole-body PET/CT scan, using low-dose CT (30 mA), were performed within the first 40 min, starting immediately after injection. At 2, 4, and 6 h after injection, an additional whole-body PET/CT scan with ultra-low-dose CT (10 mA) was performed at each time point.

MATERIALS AND METHODS

The study was conducted as a substudy within the framework of a noncommercial clinical trial (PEARL-PD; EudraCT no. 2015-003045-26) on the diagnostic use of ^{18}F-FE-PE2I in early idiopathic parkinsonism.

Participants

Five healthy volunteers (3 women, 2 men) were recruited for participation in this study via an announcement in the local newspaper. Median age was 69.6 y (range, 63–77 y). The relatively high mean age was purposely selected to match the mean age of most patients with Parkinson disease and atypical parkinsonian syndromes. The participants were in subjectively good health as confirmed by a thorough neurologic and physical examination at inclusion. The study was approved by the regional ethical review board at Umeå University, the local radiation safety committee at the University Hospital of Umeå, and the Swedish Medical Products Agency. All subjects signed an informed consent form before participation. The participants were not given any dietary restrictions.

The scanning procedures were supervised by authorized personnel, and the participants were asked to report any kind of discomfort during or after the scanning. Participants were encouraged to, if required, contact the research nurse after scanning and were followed up with a short interview by the research nurse after 14 d, to confirm the presence or absence of any possible late-onset adverse reactions.

Radiochemistry and Synthesis

^{18}F-FE-PE2I was produced at the University Hospital of Umeå according to a previously published method (*12*). Quality control was performed on each batch, including identity, chemical purity, radiochemical purity, and pH. Endotoxin and sterility testing was performed on every 20th batch or at least once every third month. All methods complied with current good manufacturing practices according to the European Pharmacopoeia.

Administered Activity

The administered activity of the ^{18}F-FE-PE2I was aimed to be 2.86 MBq/kg, with a maximum activity of 200 MBq. The dosage, 2.86 MBq/kg, was based on an administered activity of 200 MBq for a patient weighing 70 kg. The true mean administered activity per body weight of ^{18}F-FE-PE2I in this study was 2.5 MBq/kg (range, 1.8–3.1 MBq/kg), deduced from measurements of the syringe and catheter before and after injection. The participants' mean weight was 69.5 kg (range, 56–87 kg).

PET/CT Image Acquisition

The PET/CT scanning was performed at the University Hospital of Umeå on a Discovery 690 (GE Healthcare) (*13*) in 4 sessions, summarized in Figure 1. The first session, aimed to catch the fast tracer distribution, consisted of 3 head-to-thigh scans commencing at tracer injection, followed by a head-to-toe whole-body scan approximately 30 min after injection. The remaining 3 sessions were all head-to-toe scans, commencing at 2, 4, and 6 h after injection. The CT scans were acquired without x-ray modulation with 120 kV, 10 mA, and 0.5 s/revolution, except for the whole-body scan at the first session, which was acquired with 30 mA (Fig. 1) to provide good anatomic information. CT images were viewed at a 2.5-mm slice thickness. All PET scans were acquired using time-of-flight technique, with a duration of 60 s per bed position and a bed-position overlap of 11 slices. PET images, corrected for attenuation and scatter, were reconstructed using the scanner implementation of the 3-dimensional iterative ordered-subset expectation-maximization reconstruction including time-of-flight technique (VuePoint HD ViP) with 2 iterations, 24 subsets, a 6.4-mm postprocessing filter, and a 70-cm field of view, to a 128 × 128 matrix (5.5 × 5.5 × 3.27 mm voxels).

Blood and Urine Sampling

All urine was collected up to 6 h after injection. Urine from each voiding was collected in a separate bottle and measured separately. The voided volume was weighed, and the activity concentration of a 1-mL sample was measured using a well counter (NaI(Tl) scintillator) combined with a scale, so that the total voided activity could be calculated.

Venous blood samples were drawn at 40 min, 2 h, 4 h, and 6 h after injection. The activity concentrations of these samples were measured in the above-mentioned well counter. No metabolite analysis of the samples was performed, because such an analysis was beyond the scope of this dosimetry study.

Image Analysis

For image analysis and activity measurement, imlook4d (*14*), an in-house–made MATLAB (MathWorks)-based noncommercial software program, was used. The advantage of this software is that it easily allows complex volume-of-interest (VOI) delineation on images from different modalities to be merged into the PET space. It is also easily extendable, so that specialized algorithms may be developed using the MATLAB language. Using imlook4d, full-organ VOIs were delineated by one physician, double-licensed in radiology and nuclear medicine (with >15 y of clinical experience in whole-body diagnostic imaging). By combining manual drawing and segmentation techniques, we could delineate the organs for each scan. The PET and CT volumes with the best contrast were used to delineate any given organ for each individual. For instance, Hounsfield-based automatic

segmentation of the low-dose CT scan was used to create VOIs for the lungs and the spine, which were superimposed on the PET images. VOIs of some organs that could be visualized on only a few PET images were delineated using a thresholding algorithm and then transferred to the remaining PET series, after which their positions were carefully manually adjusted to anatomic markers. Transferring of VOIs between scans was done only within the same individual, followed by careful tailoring if needed. VOIs were not copied between individuals. Care was taken to avoid superposition of the VOIs with neighboring organs.

Absorbed and Effective Dose Calculation

The absorbed and effective doses were calculated using the biokinetics for each participant combined with standard phantoms (*15*). The PET images were decay-corrected to the start of the scan. The mean activity concentrations (Bq/mL) in different organs as obtained from the PET images were transformed to total activity content by multiplying by the organ masses, including blood content (g), for males or females from International Commission on Radiological Protection publication 133 (*16*). For lungs, the activity concentration was multiplied by the lung volume, which was calculated by dividing the mass by the density (0.38 g/mL). The activities were thereafter divided by the injected activity (Bq) for the specific participant to retrieve the percentage of injected activity (%IA). For bone marrow, the mean activity concentration (Bq/mL) in the spine was multiplied by the measured volume of the spine, to obtain the total amount of activity in the spine VOI. Assuming that the activity is present only in the bone marrow, we calculated the activity concentration by dividing the total activity by the literature value for the volume of active bone marrow in the spine (*15*).

For each participant, a mono- or biexponential function was fitted to the measured data using the computer program SAAM II (*17*), and the function was integrated to obtain the area under the curve, which represent the cumulated activity—that is, the mean residence time per injected activity. The software IDAC 2.0 (*18*) was used to calculate the effective dose according to International Commission on Radiological Protection publication 60 (*19*), as well as the absorbed doses to the different organs.

To obtain the residence time in the urinary bladder, the compartmental part of SAAM II was used. A 2-compartment model was created, with one compartment being the urine and the other the rest of the body. From the rest of the body, the activity could be transferred to the urine as well as out of the system. At time zero, 100% of the activity was inserted into the rest-of-body compartment, and a function was fitted to the data points of the cumulated %IA excreted with the urine. The urine compartment was thereafter adjusted to be emptied at predefined time points, as described below.

For the calculations of absorbed dose, the bladder was assumed to be voided at a 3.5-h interval, an interval used by the International Commission on Radiological Protection (*20*). To compare with a more realistic assumption, an alternative calculation was also made with the assumption that the bladder was voided 1 h after injection and thereafter at a 2-h interval (i.e., 1 h after injection, 3 h after injection, 5 h after injection, and so on).

RESULTS

Adverse Reactions

No serious adverse reactions occurred during or after the administration of the radiopharmaceutical. One participant reported a transient, swiftly resolving feeling of palpitation and vague shiver immediately after the injection of ^{18}F-FE-PE2I, without any associated objective signs. No other adverse reactions were reported during or after the PET scans.

Activity Uptake

At the early time points (10–30 min after injection), the highest activity concentration was seen in the liver (1.2, 1.1, and 1.0 %IA/100 g at 10, 20, and 30 min after injection, respectively). At later time points (1–6 h after injection), the highest activity concentration was seen in the gallbladder content (range, 1.1–0.1 %IA/100 g). At 6 h after injection, only the gallbladder, the small intestine, the salivary glands, and the red marrow showed more than 0.05 %IA/100 g. The physical decay is included in the presented values. As an example, the activity uptake at different time points after injection for participant 3 (weight, 56 kg; administered activity, 150 MBq) is displayed in Figure 2. The mean values of the activity concentration time course of several selected organs are displayed in Figure 3. PET images of all participants scanned at 1 h after injection are displayed in Supplemental Figure 1 (supplemental materials are available at http://jnm.snmjournals.org).

At the time of the first blood sample, about 40 min after injection, between 3.3 and 7.6 %IA (mean, 5.4 %IA) was found in the blood. The activity excreted in the urine during the first 6 h after injection varied between 23 and 34 %IA (mean, 28 %IA). Extrapolated data indicate that the urine was the main excretion pathway, with between 40 and 100 %IA (mean, 87 %IA; median, 100 %IA) excreted this way.

Absorbed and Effective Doses

The residence times used for the dose calculations are shown in Table 1. The mean absorbed doses per injected activity and the effective dose per injected activity are shown in Table 2. The urinary bladder received the highest absorbed dose, at 119 μGy/MBq (range, 64–200 μGy/MBq), followed by the liver, at 46 μGy/MBq (range, 31–56 μGy/MBq). The bladder contributed between 17% and 36% of the effective dose. The radiation-sensitive red

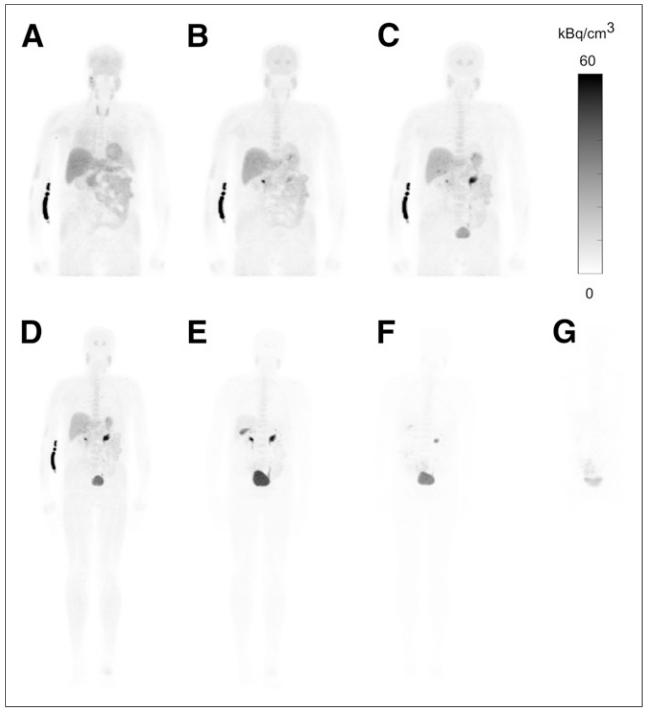

FIGURE 2. Whole-body maximum-intensity-projection images from PET scans of participant 3 at different time points after injection: 10 min (A), 20 min (B), 30 min (C), 40 min (D), 2 h (E), 4 h (F), and 6 h (G).

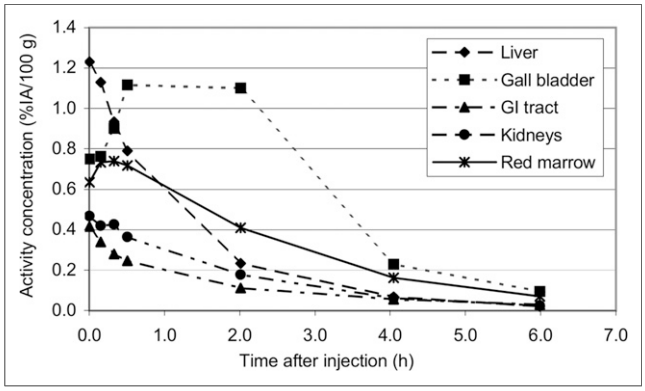

FIGURE 3. Mean activity concentration of 5 participants expressed in %IA/100 g for selection of organs. Data for gastrointestinal (GI) tract are sum of activity content (%IA) in ventricle, small intestine, and large intestine, divided by sum of the 3 organ masses (g) and multiplied by 100 g. Physical decay is taken into consideration in curves.

marrow received an absorbed dose of 25 μGy/MBq (range, 23–26 μGy/MBq).

The mean effective dose per injected activity was 23 μSv/MBq (range, 19–28 μSv/MBq), which resulted in an effective dose of 4.6 mSv for an administered activity of 200 MBq (70-kg body weight). When an alternative analysis was performed, in which the bladder was assumed to be voided more frequently, that is, at 1 h after injection and thereafter at 2-h intervals, a lower effective dose of 4.0 mSv was found. We also validated a previously published approach for ^{18}F-FE-PE2I in NHPs (*10*) in which specific uptake in the red marrow was ignored. This previous approach yielded an effective dose of 4.2 mSv (21 μSv/MBq), compared with our result of 4.6 mSv. In Table 3, the effective doses reported here are summarized with the literature values for different DAT agents and commonly used PET substances.

TABLE 1
Residence Times for Organs Used for Effective Dose Calculations

Site	Participant					Mean
	1	2	3	4	5	
Adrenals	0.001	0.002	0.002	0.001	0.001	0.001
Brain	0.029	0.054	0.063	0.040	0.049	0.047
Heart wall	0.011	0.019	0.018	0.013	0.019	0.016
Kidneys	0.015	0.036	0.041	0.023	0.027	0.028
Liver	0.154	0.374	0.410	0.209	0.252	0.280
Lungs	0.059	0.065	0.068	0.056	0.079	0.066
Pancreas	0.007	0.009	0.012	0.011	0.014	0.011
Salivary glands	0.007	0.007	0.009	0.005	0.019	0.009
Red marrow	0.237	0.220	0.251	0.249	0.202	0.232
Small intestine	0.073	0.070	0.117	0.057	0.066	0.077
Spleen	0.006	0.007	0.007	0.005	0.006	0.006
Thyroid	0.001	0.001	0.001	0.001	0.001	0.001
Ventricle wall	0.006	0.012	0.011	0.009	0.015	0.011
Bladder content	0.170	0.205	0.402	0.115	0.205	0.219
Rest of body	1.754	1.403	1.024	1.417	1.439	1.408

Data are hours.

TABLE 2
Absorbed Dose per Injected Activity

Site	Mean (n = 5)	Range
Adrenals	0.027	0.020–0.031
Bladder	0.119	0.064–0.200
Bone surfaces	0.018	0.017–0.019
Brain	0.011	0.009–0.012
Breast	0.008	0.007–0.008
Gallbladder	0.017	0.015–0.019
Gastrointestinal tract		
Stomach	0.023	0.020–0.027
Small intestine	0.028	0.023–0.035
Colon	0.015	0.013–0.016
Upper large intestine	0.015	0.014–0.016
Lower large intestine	0.014	0.013–0.016
Heart	0.018	0.014–0.019
Kidneys	0.029	0.022–0.034
Liver	0.046	0.031–0.056
Lungs	0.018	0.016–0.020
Muscles	0.010	0.009–0.010
Esophagus	0.009	0.008–0.011
Ovaries	0.015	0.014–0.017
Pancreas	0.031	0.028–0.036
Red marrow	0.025	0.023–0.026
Skin	0.007	0.006–0.007
Spleen	0.013	0.012–0.014
Testes	0.010	0.009–0.010
Thymus	0.009	0.008–0.010
Thyroid	0.013	0.012–0.013
Uterus	0.018	0.015–0.023
Salivary glands	0.019	0.010–0.037
Remaining organs	0.011	0.010–0.011
Effective dose (mSv/MBq)	0.023	0.019–0.028

Data are mGy/MBq. Doses were retrieved using IDAC 2.0. Residence times used for dose calculations are in Table 1.

DISCUSSION

The mean effective dose retrieved from the results in this study is similar to the one found by Varrone et al. in NHPs (*10*). However, there were some differences in the organ doses. The largest difference was seen in the red marrow (2.5 times higher in this study). The estimated activity in the red marrow was considered in the dose calculations in this study, whereas the red marrow in the study performed on NHPs was included in the remainder of the body. With the more refined method used in the present study, including the measurable bone marrow uptake, the effective dose

TABLE 3
Effective Dose for Selection of DAT and Amyloid Imaging Agents, as Well as ^{18}F-FDG

Agent	Effective dose per injected activity (μSv/MBq)	Injected activity (MBq)	Bladder-voiding interval (h)	Effective dose* (mSv)
^{18}F-FE-PE2I	23	200	3.5	4.6
	20	200	1 and 2	4.0
^{18}F-FE-PE2I (primates) (*10*)	21	200	4.8	4.2
^{11}C-PE2I (*22*)	6.4	222	—	1.4
^{123}I-FP-CIT (*20*)	25	185	3.5	4.6
^{11}C-PiB (*23*)	5.3	555	2.4	2.9
^{18}F-AV-45 (*24*)	18	370	2.4	6.7
^{18}F-GE067 (*25*)	34	185	2	6.3
^{18}F-BAY94–9172 (*23*)	15	300	2.4	4.5
^{18}F-FDG (*20*)	19	280	3.5	5.3

*Calculated using activity recommended for 70-kg person.

increased by approximately 10%. Also, the absorbed dose to the lungs was higher in this study, possibly because of the different species or the different methods of determining the activity uptake in lungs.

Less than 1% of free fluoride was detected during the quality controls performed on each batch. Free fluoride will be taken up in the bones, which is not the case for ^{18}F-FE-PE2I. Because of lack of free fluoride, the activity seen in the spine was assumed to be located in the red marrow and was used in the absorbed dose calculations.

In this study, the residence time for gallbladder was not estimated, and the gallbladder was included in the remainder of the body in the absorbed dose calculations. In the above-mentioned study on NHPs, the residence time for the gallbladder was included, leading to a 2.4 times higher absorbed dose to the gallbladder than found in this study. However, we do not believe that this difference affects the effective dose since the tissue-weighting factor for the gallbladder is included in the remaining organs.

Another difference between the present and the previous study is the absorbed dose to the urinary bladder, which was lower in NHPs than in humans, even though a longer voiding interval was used for the NHPs. However, in the NHPs 60%–70% of the activity was assumed to be eliminated with the urine, whereas the data in this study indicated urinary elimination close to 100%. Also, the biologic half-life of the activity transferred from the body to the urine in NHPs was assumed to be longer than what is shown in humans in this study. With a longer biologic half-life the activity has decreased more, because of physical decay, when finally arriving at the urinary bladder, leading to a decreased absorbed dose.

The absorbed dose to the bladder is a significant contributor to the effective dose. Thus, the bladder-voiding interval clearly affects the effective dose. By instructing the patient about adequate oral hydration before and after the examination and frequent voiding after the activity administration, which is part of the routine patient preparation in nuclear medicine departments, the effective dose can be reduced. In this case, the recommended voiding frequency should be at least every second hour during the rest of the day after the examination.

The effective dose per injected activity for ^{18}F-FE-PE2I is within the range of the corresponding doses for the widely used DAT imaging agent ^{123}I-FP-CIT and for other ^{18}F-labeled PET tracers, such as ^{18}F-FDG, as shown in Table 3. When the administered activity for the different substances is considered, it can be seen in Table 3 that only the ^{11}C-labeled substances result in lower effective doses than ^{18}F-FE-PE2I, because of the shorter physical half-life of ^{11}C (20 min, compared with 109 min for ^{18}F). However, the longer physical half-life of ^{18}F makes ^{18}F-FE-PE2I more easily accessible also for PET sites without an on-site cyclotron, which is needed for ^{11}C imaging.

The use of advanced image analysis software and flexible VOI tools was necessary because of the 3-dimensional and multimodal character of the collected image data in this study. In one of the participants, VOIs were initially drawn using commercial software for clinical routine PET imaging analysis installed on a GE Healthcare Advantage workstation. We compared the results derived from the VOIs drawn with the commercial software against the results from the imlook4d software in the same individual. The results were similar. However, by using the imlook4d software we gained simplicity and higher confidence in the measurements because of more accurate delineation of the organs and better reproducibility of the shapes of the VOIs between early and late scan time-points.

CONCLUSION

The effective dose per injected activity from ^{18}F-FE-PE2I was 23 μSv/MBq, similar to the previously estimated effective dose in NHPs. Thus, an administered activity of 200 MBq gives an effective dose of 4.6 mSv, which is equal to 4.6 mSv for 185 MBq of ^{123}I-FP-CIT. The lack of observed adverse events indicates that ^{18}F-FE-PE2I is safe to use in patients. The reasonable absorbed and effective doses, together with the previously reported favorable characteristics for DAT imaging and quantification, indicate that ^{18}F-FE-PE2I is a suitable radioligand for DAT imaging.

DISCLOSURE

This study was supported by grants from the Swedish Parkinson Foundation and the Västerbotten County Council (ALF). No other potential conflict of interest relevant to this article was reported.

ACKNOWLEDGMENTS

Preliminary results of this work were presented in abstract form at the Congress of European Association of Nuclear Medicine (EANM) in 2016 (*21*). We thank Helena Nylander and the staff at the Department of Nuclear Medicine at the University Hospital of Umeå for their help with conducting the PET studies. We also thank Mona Edström for her work as a coordinator.

REFERENCES

1. Darcourt J, Booij J, Tatsch K, et al. EANM procedure guidelines for brain neurotransmission SPECT using ^{123}I-labelled dopamine transporter ligands, version 2. *Eur J Nucl Med Mol Imaging.* 2010;37:443–450.
2. McKeith I, O'Brien J, Walker Z, et al. Sensitivity and specificity of dopamine transporter imaging with ^{123}I-FP-CIT SPECT in dementia with Lewy bodies: a phase III, multicentre study. *Lancet Neurol.* 2007;6:305–313.
3. Varrone A, Halldin C. New developments of dopaminergic imaging in Parkinson's disease. *Q J Nucl Med Mol Imaging.* 2012;56:68–82.
4. Politis M, Wu K, Loane C, et al. Staging of serotonergic dysfunction in Parkinson's disease: an in vivo ^{11}C-DASB PET study. *Neurobiol Dis.* 2010;40:216–221.
5. Varrone A, Tóth M, Steiger C, et al. Kinetic analysis and quantification of the dopamine transporter in the nonhuman primate brain with ^{11}C-PE2I and ^{18}F-FE-PE2I. *J Nucl Med.* 2011;52:132–139.
6. DeLorenzo C, Kumar JD, Zanderigo F, Mann JJ, Parsey RV. Modeling considerations for in vivo quantification of the dopamine transporter using [^{11}C]PE2I and positron emission tomography. *J Cereb Blood Flow Metab.* 2009;29:1332–1345.
7. Zoghbi SS, Shetty HU, Ichise M, et al. PET imaging of the dopamine transporter with ^{18}F-FECNT: a polar radiometabolite confounds brain radioligand measurements. *J Nucl Med.* 2006;47:520–527.
8. Sasaki T, Ito H, Kimura Y, et al. Quantification of dopamine transporter in human brain using PET with ^{18}F-FE-PE2I. *J Nucl Med.* 2012;53:1065–1073.
9. Fazio P, Svenningsson P, Forsberg A, et al. Quantitative analysis of ^{18}F-(*E*)-*N*-(3-iodoprop-2-enyl)-2β-carbofluoroethoxy-3β-(4′-methyl-phenyl) nortropane binding to the dopamine transporter in Parkinson disease. *J Nucl Med.* 2015;56:714–720.
10. Varrone A, Gulyás B, Takano A, Stabin MG, Jonsson C, Halldin C. Simplified quantification and whole-body distribution of [^{18}F]FE-PE2I in nonhuman primates: prediction for human studies. *Nucl Med Biol.* 2012;39:295–303.
11. Sonni I, Fazio P, Schain M, et al. Optimal acquisition time window and simplified quantification of dopamine transporter availability using ^{18}F-FE-PE2I in healthy controls and Parkinson disease patients. *J Nucl Med.* 2016;57:1529–1534.
12. Stepanov V, Krasikova R, Raus L, Loog O, Hiltunen J, Halldin C. An efficient one-step radiosynthesis of [^{18}F]FE-PE2I, a PET radioligand for imaging of dopamine transporters. *J Labelled Comp Radiopharm.* 2012;55:206–210.
13. Bettinardi V, Presotto L, Rapisarda E, Picchio M, Gianolli L, Gilardi MC. Physical performance of the new hybrid PET/CT Discovery-690. *Med Phys.* 2011; 38:5394.
14. Axelsson J. imlook4d. https://sites.google.com/site/imlook4d/. Published 2017. Accessed June 5, 2018.
15. Adult reference computational phantoms: ICRP publication 110. *Ann ICRP.* 2009;39(2).
16. Bolch WE, Jokisch D, Zankl M. The ICRP computational framework for internal dose assessment for reference adults: specific absorbed fractions—ICRP publication 133. *Ann ICRP.* 2016;45:1–74.
17. Barrett PH, Bell BM, Cobelli C, et al. SAAM II: simulation, analysis, and modeling software for tracer and pharmacokinetic studies. *Metabolism.* 1998; 47:484–492.
18. Andersson M, Johansson L, Minarik D, Mattsson S, Leide-Svegborn S. An internal radiation dosimetry computer program, IDAC 2.0, for estimation of patient doses from radiopharmaceuticals. *Radiat Prot Dosimetry.* 2014;162:299–305.
19. 1990 recommendations of the International Commission on Radiological Protection: ICRP publication 60. *Ann ICRP.* 1991;21(1–3).
20. Radiation dose to patients from radiopharmaceuticals: a compendium of current information related to frequently used substances: ICRP publication 128. *Ann ICRP.* 2015;44(2S).
21. Lizana H, Johansson L, Larsson A, et al. Dosimetry and whole body distribution of [^{18}F]PE2I in healthy volunteers [abstract]. *Eur J Nucl Med Mol Imaging.* 2016;43(suppl 1):533.
22. Ribeiro MJ, Ricard M, Lièvre MA, et al. Whole-body distribution and radiation dosimetry of the dopamine transporter radioligand [^{11}C]PE2I in healthy volunteers. *Nucl Med Biol.* 2007;34:465–470.
23. O'Keefe GJ, Saunder TH, Ng S, et al. Radiation dosimetry of beta-amyloid tracers ^{11}C-PiB and ^{18}F-BAY94-9172. *J Nucl Med.* 2009;50:309–315.
24. Lin KJ, Hsu WC, Hsiao IT, et al. Whole-body biodistribution and brain PET imaging with [^{18}F]AV-45, a novel amyloid imaging agent: a pilot study. *Nucl Med Biol.* 2010;37:497–508.
25. Koole M, Lewis DM, Buckley C, Nelissen N, Vandenbulcke M, Brooks DJ. Whole-body biodistribution and radiation dosimetry of ^{18}F-GE067: a radioligand for in vivo brain amyloid imaging. *J Nucl Med.* 2009;50:818–822.